

Grid Integrated Solar Energy Conversion System with Damped SOGI Control by Using Binary Hybrid Multilevel Inverter

B.Arikrishnan¹, R.Seven² and B.Vijayakumar³

^{1,2 &3} Students of Electrical and Electronics Engineering, Krishnasamy College of Engineering and Technology, Cuddalore

Abstract: In this paper, a damped second-order generalized integral (DSOGI) controlled binary hybrid multilevel inverter (BHMLI) driven connected to the grid solar energy converting system (SECS) is presented. The source of voltage for the inverter's H-bridge's DC-link is modified by the BHMLI architect's cascaded half-bridge arrangement producing an approximation of the reference waveform. The output waveform amplitude is improved, and the H-bridge switches' dV/dt is decreased. In transient situations, the DSOGI control reduces oscillations and overshoots and prolongs the service life of low power switches. It is used for the first time in literature in the multilayer inverter application. In addition to reducing the load's demands for harmonic and reactive power, the SECS is made to inject active power into the grid. The cascading of 'n' half-bridges and one H-bridge yield $(2(nC1) - 1)$ output voltage levels. The operation of the DC-DC converter's incremental conductance (IC) algorithm-based maximum point tracking (MPPT) allows for the maximum power extraction from solar photovoltaic (PV) arrays. It is accomplished via an isolated SIMO-SEPIC (single-input, multiple-output, single-ended primary inductance converter). The analysis of SECS with 15-level BHMLI uses both extensive simulation and a hardware prototype. Additionally, the system's shunt active filter functioning is tested under various load scenarios, and the grid power quality is maintained during operation within the IEEE-519 standard. The experimental examination at steady-state and dynamic fluctuations of load-side and insolation variations validates the theoretical assertions. The setup constructed in the lab is evaluated for a 5 kW, 400 V, three-phase system.

Keywords: Multilevel inverter, SIMO-SEPIC, solar PV, power quality.

1. INTRODUCTION

The attention is on renewable energy (RE) based power generation, which is expanding internationally at a rapid rate due to the rapid development of electrical energy consumption and the need for clean, free electricity for security of the environment. Among grid-integrated RE methods, photovoltaic (PV) solar energy systems are becoming more and more popular [1]. The key benefits of solar PV include their long lifespan, ease of installation, rooftop applications, availability of free and cheap energy, generation of clean energy, noiseless operation, lack of moving parts, and low maintenance requirements.

The efficient power transfer from the solar PV to the distribution grid with is the modern The current research direction is towards efficient power transfer from solar PV to the power distribution grid. The connected to the grid solar inverters conserve space and money by avoiding large battery banks. A typical two-level (2L) inverter-based solar power conversion device (SECS) with a modified proportional-resonant (M-PR) controller functioning in both stand-alone and grid-connected modes is reported in [2]. The main benefits are the ease of switching and circuitry. In [3], the peak-peak current ripples in the multilayer inverter (MLI) and the 2L inverter are analysed and examined, and a few pulse width modulation, or PWM strategies for lowering the current ripples are also given. The lower switching stress of 2L restricts its use to low power. Additionally, the sophisticated filters and greater switching frequency decrease efficiency and cause electromagnetic interference (EMI) problems for communication and electricity lines that are closer by.

Voltage source inverters (VSI) handle the grid-synchronization portion of SECS, and MLIs are introduced to address the drawbacks of 2L inverters. These fall into three categories: cascaded H-bridge (CHB), flying capacitor clamped (FCC), and neutral point clamped (NPC). For the first time, a three-level (3L) stacked neutral point clamped MLI's characteristics and power loss distribution are examined with solar PV applications in [4]. Although the THD is decreased, the architecture requires more switches to produce a 3L output. The literature in [5] discusses the unbalanced fault circumstances of a 3L-NPC. During a fault, the complex design or the grid's disregarded negative-sequence portion causes mistakes and delays in the power system. An FCC-MLI that concentrates on the management side of the connected to the grid power conditioning unit is disclosed in [6], [7]. The price, size, and complexity rise as the number

of capacitors and semiconductor devices increases. Unbalanced capacitor voltage is a different problem. Therefore, finding the FCC-MLI application is less appealing. A common MLI that offers a more modular topological structure and greater power transmission capabilities are CHB inverters. For larger output voltage levels and isolated DC sources, it needs a lot of switches. It is in conjunction with a SEPIC converter and is extensively utilised for PV applications, as detailed in [8].

Numerous PWM approaches have recently been published by addressing the critical power and energy balancing between the H-bridges of a CHB-MLI [9]. These days, many MLI topologies that are still as effective as ever are periodically reporting for solar power applications. The main attraction is that the management of the solar panels recognises the need for segregated DC sources in MLIs. The packed-U-cell MLI structure, which delivers good energy converting quality with fewer capacitors and power switches, is described by Kamal Al Haddad et al. For PV uses it is changed and reported in [10].

An MLI determined by two isolated 2L inverters that is connected to the grid via a three-phase transformer with open-end windings on the inverter side to realise a 3L-MLI is described in paper [11]. It is mentioned in [12] that a nine-level, connected to the grid inverter for a PV system based on two CHBs with various dc-link voltages exists. For this architecture, an additional FCC-MLI structure is required, which will result in uneven voltage levels. A secondary voltage balance circuit is therefore necessary, increasing the component count. A unidirectional switch is incorporated into the conventional CHB-MLI in a redesigned passed on connected to the grid MLI's topology [13].

Additionally, it increases the complexity of the circuit and adds more switching and conduction losses. A level doubling network and a full-bridge are coupled in series to form an asymmetrical MLI that operates under large dc-link voltage variations [14]. The total amount of levels of output voltage is increased by connecting these components. By lowering the leakage currents and increasing efficiency, a better CHB-MLI is reported in [15], and it exhibits low switching and conducting losses. A trinary DC source-based asymmetric CHB-MLI is reported in [16]. It is a 27-level MLI with a single source. A flexible multilayer single-delta bridge-cell inverter for utility-scale PV systems is presented in [17]. [18] describes an asymmetrical cascaded MLI with separate DC-DC converters powered by asymmetric power PV panels. For various panels, different maximum power point tracking (MPPT) algorithms are used. Although the output voltage levels are high, the system's dynamic performance will be slowed down by the sophisticated control. The three-level inverter is connected to a three-level step-up converter to increase power conversion efficiency by reducing voltage stress and balancing the voltages on the dc-link capacitors.

The MLI cannot self-regulate the DC bus, hence additional voltage regulation is used. Two legs make up the modified H-bridge-based MLI described in [19]: a typical two-level legs and a T-type legs. The split DC-link the halfway point is connected to the T-type, a modified 2L leg, via a bidirectional switch. A high-frequency DC-DC converter is used in an asymmetrical CHB-MLI described in [20] to generate the DC source asymmetry, which raises the overall component count, conduction losses, and system complexity. PWM is used by a hybrid nine-level MLI [21] to produce nine levels of voltage. The topology's main draw is its lower switch count of ten switches for nine levels. Because the DC-DC converter component performs the maximum power extraction and DC-link voltage stabilisation, the widely accepted two stage SECS has greater stability than single stage SECSs.

In order to link between PV and VSI, a reliable, adaptable, and straightforward DC-DC converter is required. In reference [22], a buck-boost DC-DC converter for PV applications is shown. The benefit is the wide range of voltage regulation capability. By rearranging the switching stage with a seamless transition between the modes, it only requires one buck-boost stage to regulate voltage. The Cuk, SEPIC, and Zeta converters are a novel class of converters built on capacitor links that function in the critical conduction mode [23].

To achieve zero-current and zero-voltage switching for all of the switches during the transitions, an auxiliary circuit is used. Voltage ringing across the switches, EMI problems, and dv/dt values are all minimised. Combining the switched capacitor and regenerative boost architecture results in a high gain DC-DC converter, although the number of devices is increased [24]. A boost converter operating method with a grid-connected PV system is described in [25].

2. CONFIGURATION OF GRID CONNECTED SECS

Fig. 1 depicts the three-phase solar energy conversion system's configuration. The point of common coupling (PCC) is associated with a nonlinear, unbalanced load. The PCC is also connected to an RC ripple filter to reduce voltage ripples caused by MLI switching. In SECS, a fifteen-level binary hybrid multilevel inverter is reported in this study. Three half-bridge converters (HBC) are arranged in an array and are fed in the following order: 1: 2: 4 from isolated DC sources V_1 , V_2 , and V_3 .

The H-bridge input of phase-a is V_{Ha} , and the operation of the hBC switches S_{a1} , S_{a1} , S_{a2} , S_{a2} , S_{a3} , and S_{a3} is

modulated for unipolar stepping voltage (or with low switching frequency phase shifted pulse width modulation), as illustrated in Fig. 2(a). The desired AC output voltage is produced by the H-bridge switches H_{a1} H_{a4} switched at the fundamental frequency, as shown in Fig. 2(b).

The H-bridge input of phase-a is V_{Ha} , and the operation of the hBC switches S_{a1} , S_{a1} , S_{a2} , S_{a2} , S_{a3} , and S_{a3} is modulated for unipolar stepping voltage (or with low switching frequency phase shifted pulse width modulation), as illustrated in Fig. 2(a). The required AC output voltage is produced by the H-bridge switches H_{a1} H_{a4} switched at the basic frequency, as shown in Fig. 2(b).

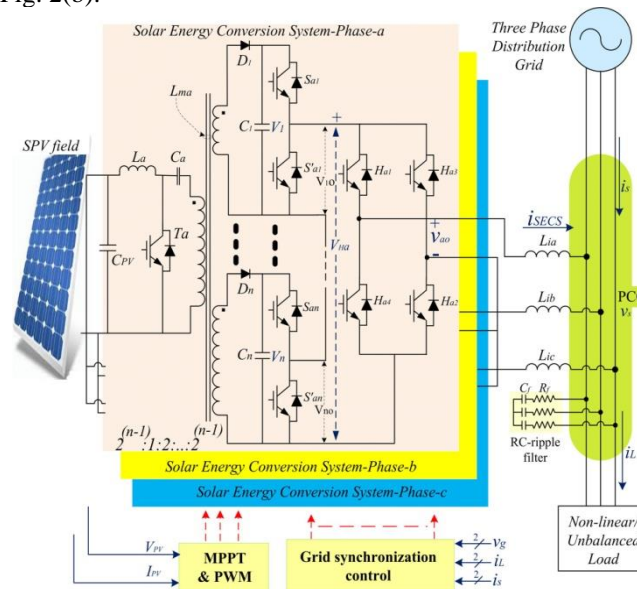


Fig.1 Circuit configuration of the solar energy conversion system.

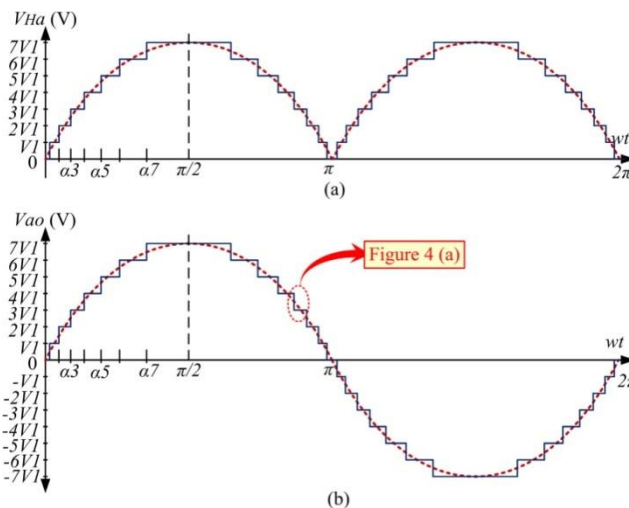


Fig 2. Expected output voltage waveforms of the SECS (a) half-bridge array output voltage V_{Ha} (b) fifteen level output voltage V_{ao} .

3. SIMULATION RESULTS AND DISCUSSIONS

This system's simulation study is done using the MATLAB/Simulink platform. The parameters of the system are shown. As seen in Fig. 3, the BHMLI produces 15-level output voltage waveforms. The peak voltage and frequency of the SECS's three-phase voltage output waveform are 325 V and 50 Hz, respectively. The system is set up so that the SECS, which is connected to the PCC and supports the irregular load demand, delivers the remaining power to the system at rated insolation (1000 W/m²). In a single frame, Fig. 4 displays the waveforms of the following parameters: irradiation level I_{rr} , PV output voltage V_{PV} , PV output current I_{PV} , output PV power P_{PV} , three-phase grid voltages vs. grid currents i_s , load currents i_L , and SECS electrical currents i_{SECS} at different conditions of operation.

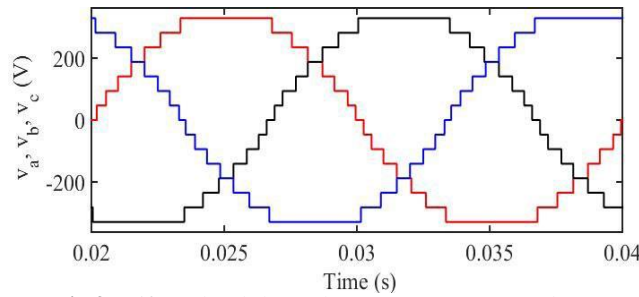
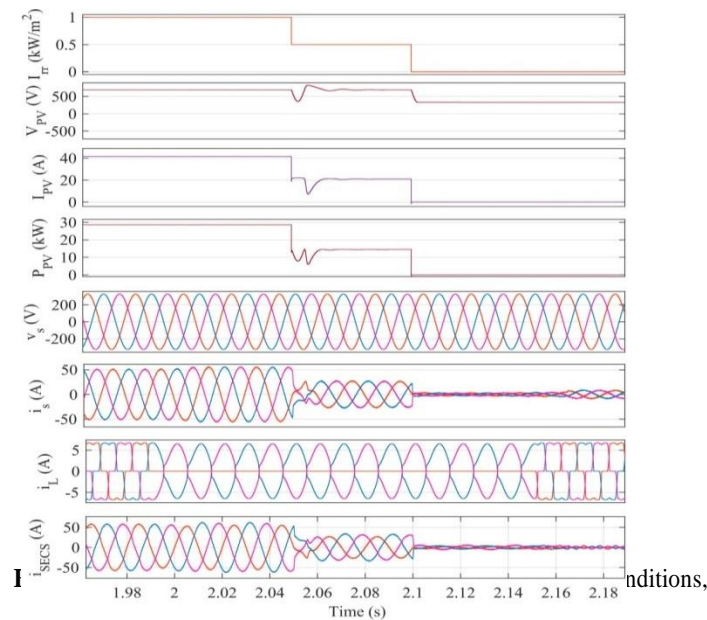


Fig 3. Fifteen level three-phase BHMLI output voltages.



I_{rr} , V_{pv} , I_{pv} , P_{pv} , v_s , i_s , i_L and i_{SECS} .

Increased grid currents. Because SECS operate unbalancedly, load single-phasing is rendered ineffective in the grid; hence, i_{SECS} are unbalanced. Within a cycle, the grid current reaches its steady state after abruptly increasing. The abrupt load reduction validates the damped controller's effectiveness by preventing any overshoots and oscillations in any area of the system. This research also shows how the system parameters are quickly achieved in a steady state. When the load is restored at 2.15 s, the performance is also observed to be satisfactory. Additionally, the grid's voltages and currents are sinusoidal and balanced.

4. EXPERIMENTAL VALIDATION

A solar energy conversion system hardware prototype is being created in the lab using a 5 kW, 400 V, 50 Hz three-phase grid-connected solar energy conversion system. After addressing the demands of the load, SECS supplies active electricity to the grid. IGBT switches with protection drivers are used to create the 15-level BHMLI, and the dSPACE Micro Lab Box 1202 is used to implement the DSOGI and MPPT controls. Digital storage oscilloscopes (DSO), scope metres, and power quality (PQ) analyzers are used to view the waveforms.

Fig. 5 shows the experimental set's BHMLI output voltage waveforms. Figure 5 (a) displays the fifteen level output voltage waveform, while Figure 5 (b) displays the uni-polar output voltage waveform at the H-bridge input VHa. The findings of an analysis of SECS performance under various load side and irradiation modifications are shown in the following sub-sections.

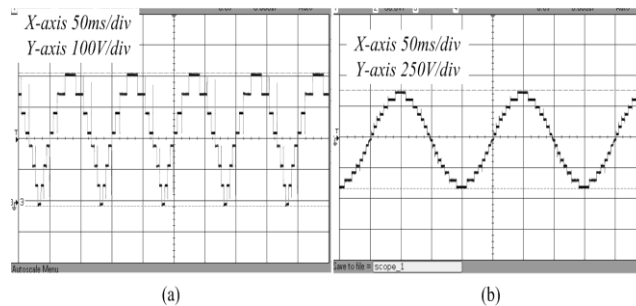


Fig 5. Fifteen-level BHMLI output voltage waveforms of phase a
 (a) V_{Ha} (b) v_{ao} .

5. CONCLUSION

In this paper, a binary hybrid multilevel inverter-based connected to the grid solar energy conversion device is designed and evaluated. Ten semiconductor switching devices and three binaries weighted independent DC-sources combine to create the fifteen-level BHMLI. The research presented here validates the benefits of reduced switching frequency, decreased device rating, and reduced component number. Damped SOGI control in BHMLI has been tested for acceptance and found to be suitable for removing overshoots and oscillations in load-related fluctuations.

REFERENCES

- [1] REN21. (2018). Renewables 2018: Global Status Report (GRS). [Online]. Available: <http://www.ren21.net/>
- [2] L. Zhang, F. Jiang, D. D. Xu, K. Sun, Y. Hao, and T. Zhang, "Two-stage transformer-less dual-buck PV grid-connected inverters with high efficiency," *Chin. J. Elect. Eng.*, vol. 4, no. 2, pp. 36–42, Jun. 2018.
- [3] J.-S. Kim, J.-M. Kwon, and B.-H. Kwon, "High-efficiency two-stage three-level grid-connected photovoltaic inverter," *IEEE Trans. Ind. Electron.*, vol. 65, no. 3, pp. 2368–2377, Mar. 2018.
- [4] Y. Wang and F. Wang, "Novel three-phase three-level-stacked neutral point clamped grid-tied solar inverter with a split phase controller," *IEEE Trans. Power Electron.*, vol. 28, no. 6, pp. 2856–2866, Jun. 2013.
- [5] T. Jin, H. Wei, D. L. M. Nzongo, and Y. Zhang, "Model predictive control strategy for NPC grid-connected inverters in unbalanced grids," *Electron. Lett.*, vol. 52, no. 14, pp. 1248–1250, Jul. 2016.
- [6] K. Hemici, A. Zegaoui, A. A. Bokhtache, M. O. Mahmoudi, and M. Aillerie, "Three-phases Flying-capacitor multilevel inverter with proportional natural PWM control," in *Proc. Int. Conf. Technol. Mater. Renew. Energy, Environ. Sustainability*, 2015, pp. 1061–1070.
- [7] M. Trabelsi, K. A. Ghazi, N. Al-Emadi, and L. Ben-Brahim, "A weighted real-time predictive controller for a grid connected flying capacitors inverter," *Int. J. Elect. Power Energy Syst.*, vol. 49, pp. 322–332, Jul. 2013.
- [8] C. M. Nirmal Mukundan and P. Jayaprakash, "Solar PV fed cascaded H-bridge multilevel inverter and SIMO-SEPIC based MPPT controller for 3-phase grid connected system with power quality improvement," in *Proc. Nat. Power Electron. Conf. (NPEC)*, Pune, India, 2017, pp. 106–111.
- [9] A. S. Gadalla, X. Yan, S. Y. Altahir, and H. Hasabelrasul, "Evaluating the capacity of power and energy balance for cascaded H-bridge multilevel inverter using different PWM techniques," *J. Eng.*, vol. 2017, no. 13, pp. 1713–1718, Jan. 2017.
- [10] H. Vahedi, M. Sharifzadeh, and K. Al-Haddad, "Modified seven-level pack U-Cell inverter for photovoltaic applications," *IEEE J. Emerg. Sel. Topics Power Electron.*, vol. 6, no. 3, pp. 1508–1516, Sep. 2018.
- [11] G. Grandi, C. Rossi, D. Ostojic, and D. Casadei, "A new multilevel conversion structure for grid-connected PV applications," *IEEE Trans. Ind. Electron.*, vol. 56, no. 11, pp. 4416–4426, Nov. 2009.
- [12] G. Buticchi, D. Barater, E. Lorenzani, C. Concarri, and G. Franceschini, "A nine-level grid-connected converter topology for single-phase transformerless PV systems," *IEEE Trans. Ind. Electron.*, vol. 61, no. 8, pp. 3951–3960, Aug. 2014.
- [13] F. Wu, X. Li, F. Feng, and H. B. Gooi, "Modified cascaded multilevel grid-connected inverter to enhance European efficiency and several extended topologies," *IEEE Trans. Ind. Informat.*, vol. 11, no. 6, pp. 1358–1365, Dec. 2015.
- [14] S. K. Chattopadhyay and C. Chakraborty, "A new asymmetric multi-level inverter topology suitable for solar PV applications with varying irradiance," *IEEE Trans. Sustain. Energy*, vol. 8, no. 4, pp. 1496–1506, Oct. 2017.
- [15] S. Jain and V. Sonti, "A highly efficient and reliable inverter configuration based cascaded multilevel inverter for PV systems," *IEEE Trans. Ind. Electron.*, vol. 64, no. 4, pp. 2865–2875, Apr. 2017.
- [16] M. S. Manoharan, A. Ahmed, and J.-H. Park, "A PV power conditioning system using nonregenerative single-

sourced trinary asymmetric multi-level inverter with hybrid control scheme and reduced leakage current,” IEEE Trans. Power Electron., vol. 32, no. 10, pp. 7602–7614, Oct. 2017.

[17] P. Sochor, N. M. L. Tan, and H. Akagi, “Low-voltage-ride-through control of a modular multilevel single-delta bridge-cell (SDBC) inverter for utility-scale photovoltaic systems,” IEEE Trans. Ind. Appl., vol. 54, no. 5, pp. 4739–4751, Sep. 2018.

[18] M. K. Das, K. C. Jana, and A. Sinha, “Performance evaluation of an asymmetrical reduced switched multi-level inverter for a grid-connected PV system,” IET Renew. Power Gener., vol. 12, no. 2, pp. 252–263, Feb. 2018.

[19] G. E. Valderrama, G. V. Guzman, E. I. Pool-Mazun, P. R. Martinez-Rodriguez, M. J. Lopez-Sanchez, and J. M. S. Zuniga, “A single-phase asymmetrical T-type five-level transformerless PV inverter,” IEEE J. Emerg. Sel. Topics Power Electron., vol. 6, no. 1, pp. 140–150, Mar. 2018.

[20] A. Ahmed, M. Sundar Manoharan, and J.-H. Park, “An efficient single-sourced asymmetrical cascaded multilevel inverter with reduced leakage current suitable for single-stage PV systems,” IEEE Trans. Energy Convers., vol. 34, no. 1, pp. 211–220, Mar. 2019.

[21] C. Phanikumar, J. Roy, and V. Agarwal, “A hybrid nine-level, 1- ϕ grid connected multilevel inverter with low switch count and innovative voltage regulation techniques across auxiliary capacitor,” IEEE Trans. Power Electron., vol. 34, no. 3, pp. 2159–2170, Mar. 2019.

[22] A. Chub, D. Vinnikov, R. Kosenko, and E. Liivik, “Wide input voltage range photovoltaic microconverter with reconfigurable buck-boost switching stage,” IEEE Trans. Ind. Electron., vol. 64, no. 7, pp. 5974–5983, Jul. 2017.

[23] M. Khodabandeh, E. Afshari, and M. Amirabadi, “A family of \acute{C} uk, Zeta, and SEPIC based soft-switching DC–DC converters,” IEEE Trans. Power Electron., vol. 34, no. 10, pp. 9503–9519, Oct. 2019.

[24] V. Karthikeyan, S. Kumaravel, and G. Gurukumar, “High step-up gain DC–DC converter with switched capacitor and regenerative boost configuration for solar PV applications,” IEEE Trans. Circuits Syst. II, Exp. Briefs, vol. 66, no. 12, pp. 2022–2026, Dec. 2019.

[25] L. V. Bellinaso, H. H. Figueira, M. F. Basquera, R. P. Vieira, H. A. Grundling, and L. Michels, “Cascade control with adaptive voltage controller applied to photovoltaic boost converters,” IEEE Trans. Ind. Appl., vol. 55, no. 2, pp. 1903–1912, Mar. 2019.